Journal of Polymers and the Environment
https://doi.org/10.1007/s10924-019-01536-6

ORIGINAL PAPER

Autoxidized Oleic Acid Bifunctional Macro Peroxide Initiators for Free Radical and Condensation Polymerization. Synthesis and Characterization of Multiblock Copolymers

Baki Hazer[1,2,3] · **Elif Ayyıldız**[3] · **Melike Eren**[2] · **Hale Seçilmiş Canbay**[4] · **Richard D. Ashby**[5]

Abstract

Autoxidation of unsaturated fatty acids gives fatty acid macroperoxide initiators containing two functionalities which can lead to free radical and condensation polymerizations in a single pot. The oleic acid macroperoxide initiator obtained by ecofriendly autoxidation (Pole4m) was used in both the free radical polymerization of styrene and the condensation polymerization with amine-terminated polyethylene glycol (PEGNH2) to obtain triblock branched graft copolymers. The narrow molar masses of the poly oleic acid-g-styrene (PoleS) and poly oleic acid-g-styrene-g-PEG (PoSG) graft copolymers were successfully obtained. The inclusion of oleic acid decreased the glass transition temperature of the polystyrene segment because of the plasticizing effect of oleic acid. In addition, a mechanical property of the copolymer was improved when compared with the pure PS. Structural characterization, morphology of the fracture surface, micelle formation, thermal analysis and molar masses of the obtained products were also evaluated.

Keywords Oleic acid · Macroperoxide initiator · Autoxidation · Amphiphilic copolymer

Introduction

Polymeric materials obtained from renewable natural resources are now being accepted as 'biobased polymers'. Current efforts are focused on the use of renewable resources to prepare biobased materials because of environmental issues and limited fossil raw materials [1–3].

Vegetable oils are commercially available renewable raw materials that can be used to produce thermosets, plastics and elastomers [4–10]. In addition, soybean oil polyols were used as monomers to synthesize polyurethane with different reactants [11, 12].

Autoxidation is the reaction of polyunsaturated fatty acids/plant oils with air oxygen. Autoxidation starts with hydrogen abstraction from the allylic methylene group which causes radical formation on the carbon atom. Oxidation reactions of the unsaturated vegetable oils can result in the formation of epoxides, peroxides and hydroperoxide derivatives depending on the specific reaction conditions [13–18]. Oxygen is then attached to this radical to form hydroperoxide and/or peroxide groups which can be converted to hydroxyl groups at elevated temperature [19] using either a reducing agent [20], a catalyst [21–23], or by the reaction with diethanolamine [24].

The effect of gold [25] and silver [26] nanoparticles on the autoxidation process of soybean oil has been studied in detail. Autoxidation was strongly catalyzed by gold nanoparticles while silver nanoparticles did not show any catalytic effect on the autoxidation process. Peroxide derivatives of soybean oil can initiate free radical olefin polymerization as a macroperoxide initiator, because a macroinitiator is a

✉ Baki Hazer
bkhazer@beun.edu.tr

✉ Richard D. Ashby
rick.ashby@ars.usda.gov

[1] Department of Aircraft Airframe Engine Maintenance, Kapadokya University, 50420 Ürgüp, Nevşehir, Turkey

[2] Department of Chemistry, Faculty of Engineering, Faculty of Arts and Sciences, Bülent Ecevit University, 67100 Zonguldak, Turkey

[3] Department of Nano Technology Engineering, Faculty of Engineering, Bülent Ecevit University, 67100 Zonguldak, Turkey

[4] Bioengineering Department, Mehmet Akif Ersoy University, 15030 Burdur, Turkey

[5] USDA ARS, East. Reg. Res. Ctr, 600E Mermaid Lane, Wyndmoor, PA 19038, USA

macromolecule containing functional group(s) that can initiate polymerization of a monomer such as macroazo initiators [27–29] and macroperoxide initiators [30, 31].

Linolenic and linoleic acids typically found in polyunsaturated plant oils also produce peroxide oligomers via autoxidation. These peroxide derivatives were used as macroperoxide initiators in order to start the free radical polymerization of vinyl monomers leading to graft copolymers [32, 33]. Recently, an oleic acid macroperoxide initiator was obtained by autoxidation [34] and then used along with an amine-terminated polyethylene glycol (PEGNH2) in a one-pot polymerization of N-isopropyl acryl amide to obtain a thermo responsive double hydrophilic polymer with a lower critical solution temperature.

PEG is water soluble polymer. It has been finding a wide range application in industry and medicine. Therefore, there are many PEG based copolymer reported as homopolymer and copolymer form [35–40].

Lately, one pot polymerization reactions have become attractive. The benefits of one pot polymerizations are that different block co-polymers can be produced without the need for purifying intermediates, which saves time and resources and thus provides easy access to polymers with various functionalities and architectures [41–43]. This might be associated with combination polymerization reactions such as reactions of cationic to free radical polymerizations in order to prepare block/graft copolymers [44–47].

The motivation of this work was to gain a better understanding of the polymerization of oleic acid macroperoxide initiator and the characterization of the products. In the present work, we report a novel one pot synthesis of copolymer via the combination of free radical polymerization of styrene and amidation condensation reactions. Oleic acid macroperoxide (Pole) obtained previously in our laboratory was used in this work. It was structurally characterized by means of the molar mass, C, H elemental analysis and iodine index. Then, the poly(oleic acid-g-styrene-g-PEG) graft copolymer was synthesized by using the mixture containing styrene, PEGNH2 and Pole. Physicochemical and thermal characterizations of the obtained copolymer were performed.

Experimental

Materials

Diamine-terminated polyethylene glycol with MW ~ 2000 g/mol (Jeffamine D-2003; PEG2KNH2) and (O, O′-bis (2-aminopropyl) polypropylene glycol–block polyethylene glycol–block-polypropylene glycol) were gifts from Huntsman Co. (Istanbul). The mole ratio of ethylene glycol units to propylene glycol units was 36/9. Oleic acid (purity: 85–88 wt %) was kindly gifted from “CHS Endüstriyel Ürünler San. Tic. A.Ş. Büyükdere Caddesi No: 122 A Blok Kat:2 Esentepe İstanbul”. Stannous octanoate (Sn-oct) and Tetrahydrofuran (THF) with butylated hydroxytoluene (BHT) were supplied from Sigma-Aldrich (Germany). To prevent the inhibition period, styrene was passed in alumina bed, which absorbs water and t-butyl catechol according to the cited articles [48, 49].

Autoxidized Polymeric Oleic Acid (Pole4m)

Autoxidation of oleic acid was performed according to the modified procedure reported in a recent work [34]. Briefly, 18 g of oleic acid was spread out into a Petri dish ($\Phi = 14.5$ cm, oil thickness: 1.1 mm) where it was exposed to daylight in the air at room temperature. After 4 months, a sticky, pale yellow viscous liquid polymer layer was formed. ^{1}H NMR ($CDCl_3$), δ_{ppm} from TMS, 11.2 (s, –COO**H**), 5.3 (s, –**CH**=**CH**–), 3.6 and 3.9 (m, –**CH**–O–s), 2.3 (t, –$\mathbf{CH_2}$–COOH), 2.0 (m, –$\mathbf{CH_2}$–CH_2–COOH), 1.3 and 1.6 (m, the rest of –$\mathbf{CH_2}$–s), 0.9 (t, $\mathbf{CH_3}$–).

Iodine Number

The Wijs method [50] was used to determine the iodine value of the oxidized oleic acid. Iodine monochloride was used for the double-bond addition reaction, and the consumed iodine was measured by back titration with 0.1 M standard sodium thiosulfate solution. Sample weight was taken around 0.2 g and the iodine number was calculated using Eq. 1.

$$\text{Iodine Number} = \frac{(\text{Blank Titer} - \text{Sample Titer, mL})(0.01269)(100)}{\text{Sample Wt., g}} \qquad (1)$$

Fractionation of the Oxidized Samples

Fractionation of the oxidized oleic acid was performed by the procedure for autoxidized soybean oil described in our recent study [25]. The crude oxidized oleic acid polymer (40 g) was dissolved in 20 mL of $CHCl_3$. Then, 800 mL of petroleum ether was added to this solution. After stirring for 2 h, the mixture was kept at 4 °C overnight. The upper phase was decanted, the precipitate was leached with petroleum ether and then the resulting upper solution was decanted. The precipitate was dried under vacuum at room temperature for 24 h. The petroleum ether phases were combined, and the solvent was evaporated. The precipitate was dried in a vacuum oven at room temperature for 24 h and kept as the main fraction. The molar mass of the oleic acid macroperoxide was determined using size exclusion chromatography (SEC or GPC). Molar mass (Mn) of the main fraction of Pole4m was found to be 1760 g/mol with the poly dispersity

(Đ) 1.03 indicating that Pole4m was composed of 6 oleic acid repeating units. The yield was 95 wt%.

Copolymerization of Styrene and Pole4m (PoleS)

Free radical polymerization of styrene was initiated by Pole according to the modified procedure described in the cited literature [25]. For a typical polymerization experiment, Pole4m (0.050 g, 0.028 mmol) and styrene (4.52 g, 45.2 mmol) were dissolved in 5 mL of toluene in a reaction bottle. Argon was introduced through a needle into the tube for about 3 min to expel the air. The tightly capped bottle was then put into a water bath at 95 °C for 6 h. The content of the bottle was poured into methanol (200 mL) under vigorous stirring. The precipitated graft copolymer was dried overnight under vacuum at 30 °C. Polymer films (approximately 0.5 mm thickness) were cast from the chloroform solutions (approximately 0.50 g of polymer sample in 15 mL chloroform) in a Petri dish ($\Phi = 5.0$ cm) covered with a piece of paper. ^{1}H NMR ($CDCl_3$), δ_{ppm} from TMS, 6.5–7.2 (m, –benzene rings), 1.2–1.9 (m, aliphatic protons both PS and Pole), 0.9 (t, $C\mathbf{H}_3$– of Pole).

Condensation Reaction Between PoleS and PEGNH2 [Poly(oleic acid-g-styrene-g-PEG)]

For a typical reaction, a mixture of PoleS (0.656 g), Sn-oct (0.10 g) PEGNH2 with a molecular weight of 2000 g/mol (0.624 g) and was dissolved in 30 mL of $CHCl_3$. The solution was filtered through small impurities into a Petri dish ($\Phi = 7$ cm) which was loosely covered with a piece of cardboard to allow the solvent to evaporate slowly for 48 h. The resultant film was covered with aluminum foil and kept at 110 °C under vacuum for 2 h. Purification was accomplished by dissolving the crude graft copolymer film in 10 mL of chloroform and precipitating the polymers in 200 mL of methanol. The purified polymers were dried at 40 °C under vacuum for 24 h. ^{1}H NMR ($CDCl_3$), δ_{ppm} from TMS, 6.5–7.2 (m, –benzene rings), 3.6 (–$C\mathbf{H}_2$–$C\mathbf{H}_2$–O–), 1.2–1.9 (m, aliphatic protons both PS and Pole), 0.9 (t, $C\mathbf{H}_3$– of Pole).

One Pot Synthesis of Amphiphilic Copolymer, Poly(oleic acid-g-styrene-g-PEG)

The combination of free radical and condensation polymerization was used to prepare the final terpolymer. The mixture of 2.0 g of styrene (0.02 mol), 2.0 g of Pole and 2.0 g of PEGNH2 was dissolved in 5 mL of toluene in a glass bottle. Argon was introduced through a needle into the tube for about 3 min to expel the air. The tightly capped bottle was then put into a water bath at 95 °C for 5 h. Then, the solvent was evaporated and the crude polymer was precipitated in 200 mL of methanol. The graft copolymer samples were dried under vacuum at 40 °C for 24 h. ^{1}H NMR ($CDCl_3$), δ_{ppm} from TMS, 6.5–7.2 (m, –benzene rings), 3.6 (–$C\mathbf{H}_2$–$C\mathbf{H}_2$–O–), 1.2–1.9 (m, aliphatic protons both PS and Pole), 0.9 (t,$C\mathbf{H}_3$– of Pole).

Determination of Water Uptake

First, solvent-cast polymer films from tetrahydrofuran (THF) solution were prepared. 1.0 g of polymer was dissolved in 20 mL of THF. The solution was filtered from small impurities into a Petri dish (F = 5 cm). The Petri dish was covered with a piece of clean cardboard for the slow evaporation of the solvent. Any polymer films that stuck together in the Petri dish were soaked in distilled water for several hours to separate them. Water uptake was determined by soaking the films in water for 48 h. The swollen films were removed from the water, gently wiped with a paper tissue and weighed. The films were then dried under vacuum at 60 °C for 24 h. The water uptake of the film was calculated using the following equation:

$$\text{Water uptake (wt\%)} = \frac{m_s - m_d}{m_d} \times 100 \tag{2}$$

where, m_s is weight of swollen polymer film and m_d is weight of dried polymer film.

Characterization

Molecular weights were determined by size exclusion chromatography. A Viscotek GPCmax system was used, consisting of a pump, three ViscoGEL GPC columns (G2000H HR, G3000H HR and G4000H HR), and a Viscotek differential refractive index (RI) detector. Tetrahydrofuran (THF) with a flow rate of 1.0 mL/min at 30 °C was used. A calibration curve was generated with three polystyrene (PS) green standards: 2960, 50,400, and 696,500 Da, of low polydispersity. The polymer sample solutions containing 0.05 g in 10 mL of THF were filtered from small impurities and injected automatically into the instrument. Data was analyzed using Viscotek Omni SEC Omni 01 software.

Proton NMR spectra in $CDCl_3$ were taken at a temperature of 25 °C with an Agilent 600 MHz NMR (Agilent, Santa Clara, CA, USA) spectrometer equipped with a 3 mm broadband probe. FT-IR spectra of the polymer samples were recorded using Perkin-Elmer FT-IR Spectrometer 100 equipped with a single diamond ATR in transmissive mode and scan rate 4000 to 650 cm^{-1}.

DSC analyses of the polymers were performed under nitrogen (flow rate = 50 mL/min.) using a Perkin Elmer DSC 4000 instrument. The dried samples were heated from -50 to 190 °C at a heating rate 10 °C/min. Thermogravimetric

Analysis (TGA) was carried out in a TGA-DTA instrument: Seiko SIITG/DTA 7200. Weight loss of the samples under nitrogen atmosphere was measured by heating each sample from 20 to 600 °C at a heating rate 10 °C/min.

Carbon and Hydrogen elemental analysis of the oleic acid macroperoxide and the pure oleic acid were carried out using a LECO, CHNS-932 elemental analysis instrument. Each measurement was repeated twice using 10 mg of sample and the results were taken in average of two measurements for each sample.

Fracture surface analysis was carried out with an SEM Quanta FEG 450 (FEI) instrument with EDS analysis SDD APOLLO X (EDAX). Samples were coated with a Au film and the SEM images were obtained using a secondary electron detector (ETD). Surface morphology of polymer samples was examined by a field-emission scanning electron microscope operated at 15–25 kV.

Micelle formation was observed using transmission electron microscopy (TEM). 10 mg of sample was dissolved in 10 mL of THF. Distilled water was gradually added into this solution with continuous stirring until the turbid solution was obtained. Then, the solution was put in an ultrasonic bath for 10 min. The TEM sample preparation was performed by placing a solution (1 to 2 drops) on 200-mesh carbon-coated copper TEM grid (EMS CF200-Cu). The TEM measurements were conducted using a JEOL JEM-2100 HRTEM instrument at 200 kV (LaB6 filament). The elemental analyses were carried out with an Oxford Instrument with a 6498 energy dispersive spectroscopy (EDS) system. The images were recorded using a slow scanning CCD camera (Gatan-694 model) with Gatan Digital Micrograph software.

Stress–Strain Measurements

A Zwick/Roell Tensile Testing Machine using a 50 kg load cell and a crosshead speed of 50 mm/min was used for stress–strain measurements. Films were solvent-cast from $CHCl_3$ at 24 °C and cut into rectangles with dimensions of 0.50 × 10 × 50 mm. Samples were dried at room temperature under vacuum for 10 days prior to measurement. At least three samples from each blend composition were measured.

Results and Discussion

Synthesis of Oxidized Oleic Acid Polymer

The oleic acid macroinitiator obtained after 4 months of oxidation (Pole4m) was used in this work. Oxygen uptake is typically related to the number of double bonds in the fatty acid molecules. This suggests that the amount of oxygen uptake should proceed from linolenic acid > linoleic acid > oleic acid. In our studies, oleic acid did, in fact, show the slowest autoxidation compared to both linolenic acid and linoleic acid which agrees well with previously reported results [17, 34].

The oxidation process was explained in detail in a recently published article [34]. In short, oxidation was carried out by the reaction of oleic acid with the oxygen present in air under daylight at room temperature. During the autoxidation process, oxygen attacks the allylic hydrogen causing hydrogen abstraction leading to radical formation at the carbon atom [51, 52].

Oxygen molecules are then attached to this carbon to form hydroperoxides and/or peroxides. Oleic acid macroperoxide with 6 oleic acid repeating units was obtained via autoxidation of oleic acid (thickness = 1 mm, oxidation time = 4 months). In this work, oleic acid macroperoxide (coded as: Pole4m) was used because the longer autoxidation time resulted in a higher molar mass of the oleic acid macroperoxide initiator (1760 g/mol) making it possible to insert a large amount of the polyoleic acid units into the graft copolymer improving the plasticizing effect. The multiblock graft copolymer can be designed as shown in Fig. 1.

Structural characterization of Pole was performed using ^1H NMR spectroscopy the results of which can be seen in our recent article [34]. The characteristic signals of pure oleic acid [53]were observed in the ^1H NMR spectrum of Pole4m with the additional signals of –CH–OO– at 3.5–4.1 ppm. As expected, the intensity of the signal of the allylic protons at 2.0 ppm decreased because of the hydrogen abstraction during the autoxidation to form peroxide and hydroperoxide groups.

Iodine value is a measure of the degree of unsaturation within the oil. The iodine index value of Pole was found to be 75 while pure oleic acid was 95. This may be attributed to some double bonds undergoing additional side reactions such as aldehyde formation [54]. In addition, the fatty acids do not undergo Diels–Alder reactions [55] in the absence of an aggressive electrophilic diene. In order to determine the peroxide decomposition of the oxidized oleic acid macroperoxide (Pole4m), DSC analysis was used. Figure 2 shows a DSC curve of Pole4m. A slight exothermic decomposition was observed. The weak peroxide decomposition of the Pole4m started from 134 °C to 188 °C. In addition to this, glass transition (T_g^{onset}) was also observed at 14 °C for the oleic acid macroperoxide, Pole4m.

In addition to this, comparison of C and H elemental analysis results of the Pole (wt%) (C: 69.75; H: 10.81; O: 19.44) and pure oleic acid result (C: 77.14; H: 11.42; O: 11.44). Considering the molar mass of Pole4m 1760 g/mol, oxygen uptake was found to be 140.56 g per mol. This is equal of 4.4 peroxy groups per molecule of Pole.

Fig. 1 Schematic design of one pot synthesis of PS-g-Pole-g-PEG graft copolymer

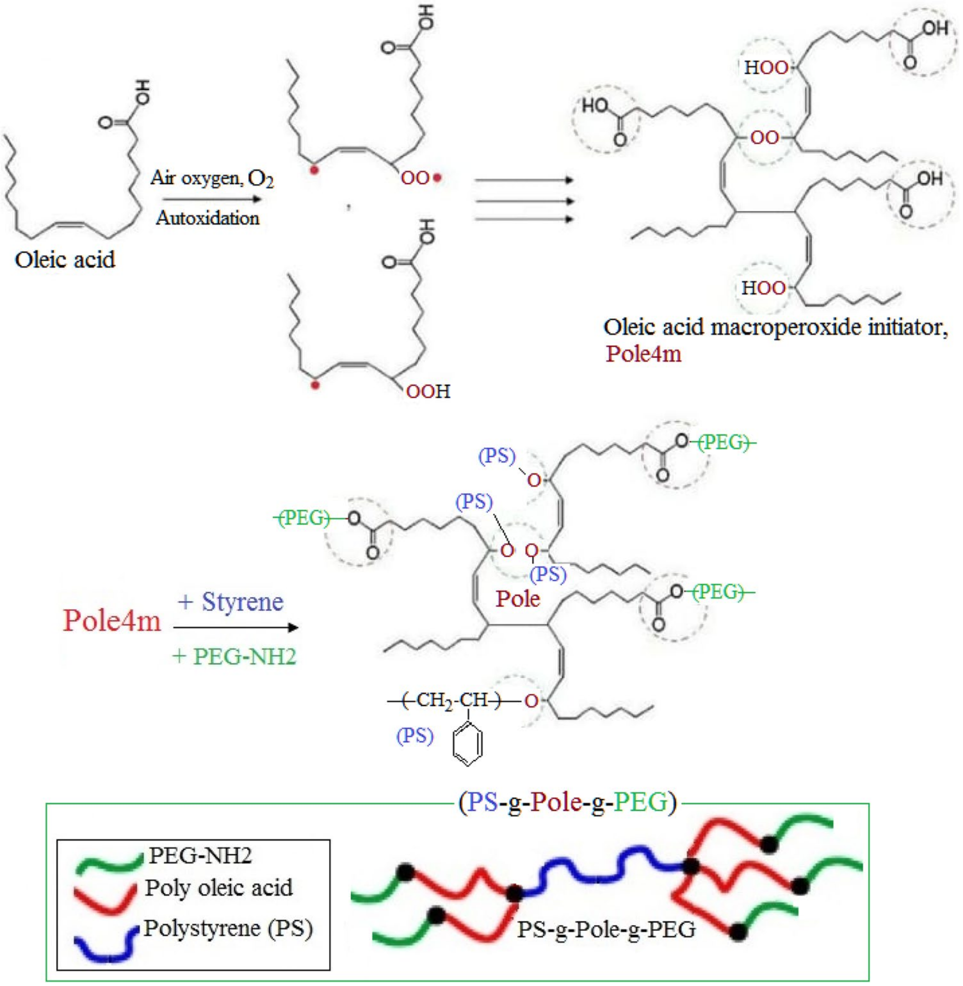

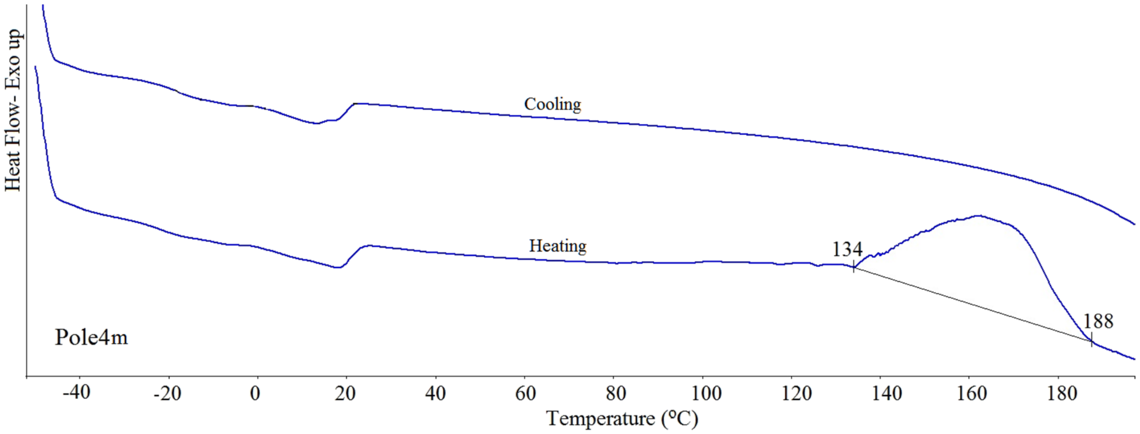

Fig. 2 DSC curve of Pole4m. Decomposition of the peroxide groups starts from 134 and ends at 188 °C

Polymerization of Styrene Initiated by Pole

The increasing initial concentration of Pole in the free radical polymerization of styrene caused a decrease in the molar masses of the polymers as shown in Fig. 3. Polydispersity index (Đ) of the PoleS samples varied from 1.41 to 1.50. This shows that the free radical polymerization of styrene initiated by Pole resulted in low Đ polymers. The uniformity

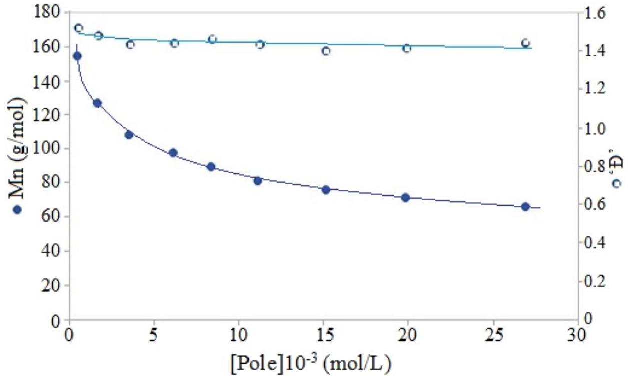

Fig. 3 The variation of molar masses and against the concentration of Pole4m

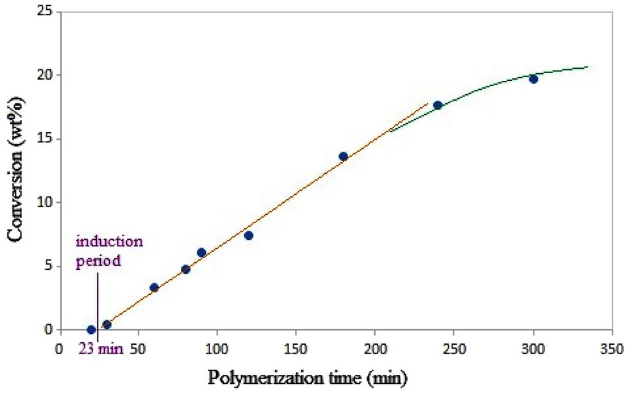

Fig. 4 Time-conversion plot for the free radical polymerization of styrene initiated by Pole4m

amongst the molar masses of the polymers described here are comparable with the results reported in the controlled living radical polymerization [56]. Controlled living radical polymerization leads to polymers with low polydispersity. However the conventional radical polymerization in this work also gave the polymers with low polydispersity. Then we can conclude that the free radical polymerization initiated with oleic acid macroinitiator, Pole, is competitive with controlled living polymerization.

Effect of the Polymerization Time on the Conversion

In order to see the conversion against polymerization time, an experimental series of styrene polymerization in toluene initiated by Pole4m was carried out at 95 °C. In these experiments, yield of thermal polymerization of styrene was subtracted from the polymer yield. Interestingly, we observed a 23 min induction period prior to initiating polymerization. The linear time-conversion plot is shown in Fig. 4.

Bulk Polymerization of Styrene Initiated by Pole4m

The same solution polymerization technique was used in the free radical polymerization initiated by Pole4m without the solvent. The polymerization results and conditions are shown in Table 1.

In those reactions the bulk polymerization of styrene was initiated by Pole4m by changing the molarity between 0.06 M and 0.29 M. PoleS graft copolymers were obtained in moderate molar masses with 'Đ' values between 1.47 and 2.06. The molar masses of the graft copolymers were found to be clearly lower at higher initiator concentrations. The molar masses decrease when initiator concentration increase because termination increase. We used these PoleS graft copolymers in chain extension reactions as described in the next section.

Multiblock Copolymers Using PoleS diblock Copolymer

When DSC analysis of Pole3S was taken, we observed that Pole3S contained undecomposed peroxide which decomposition starts from 130 °C to 184 °C. Figure 5 shows the DSC curve of Pole3S with a heating curve and a cooling curve. These copolymers are all amorphous because main polymer matrice is amorphous PS. The unreacted peroxide residue in the polymer chain thermally is cleaved producing radical moieties that attach to unsaturated groups in order to form block/graft copolymers [57, 58]. In the second cycle, this situation is seen with a smooth line and the decomposition curve disappears.

This diblock copolymer was then used in the free radical polymerization of n-BMA to obtain multiblock copolymers.

Table 1 The bulk polymerization results and conditions of styrene initiated by Pole4m (95 °C, 5 h)

Code	Pole4m		S		Yield	Mn	Mw	'Đ'
	(g)	[M]	(g)	[M]	(wt%)	(g/mol)	(g/mol)	
PoleS-2–18	2.0	0.06	18.1	8.7	58.7	36,100	53,000	1.47
PoleS-6–14	6.0	0.17	14.1	6.7	63.2	19,400	32,300	1.66
PoleS-11–9	11	0.31	9.4	4.5	39.5	10,900	18,600	1.71
PoleS-25–14	25	0.29	14.0	3.5	19.2	9400	19,000	2.06
Pole3S	3.0	0.17	7.3	7.0	50.1	24,700	44,300	1.79

Table 2 shows the results and conditions of the free radical polymerization of n-BMA initiated by PoleS diblock copolymer.

Chain Extension by the Reaction of PoleS with PEGNH2

In this work, we established a series of condensation reactions between PoleS and PEGNH2. The two amine terminals of PEG influenced the chain extension during the condensation reactions between PoleS and PEGNH2. Lower equivalency of diamine terminated PEG leads to the higher molar masse of polymers without any crosslinking. If equivalency is settled according to the functional groups, cross-linked polymers can be obtained. In this time, cross-linking may occur at the end of the very long polystyrene chains.

The results and conditions of the condensation reactions between PoleS and PEGNH2 were tabulated in Table 3. These results showed that the condensation reaction of polystyrene-oleic acid graft copolymers with diamine-terminated PEG leads to the chain extension. A noticeable increase in molar mass was observed in run PoleS2514PEG-3. The multi block copolymer with Mn 54,400 g/mol was obtained using the starting diblock copolymer with Mn 9400 g/mol. An ammonium carboxylate salt was formed when the carboxylic acid functionalized PoleS sample was mixed with PEG containing primary amine ends in dichloromethane. After the solvent was evaporated, the crude carboxylated ammonium salt was cured under vacuum at 110 °C for 2 h.

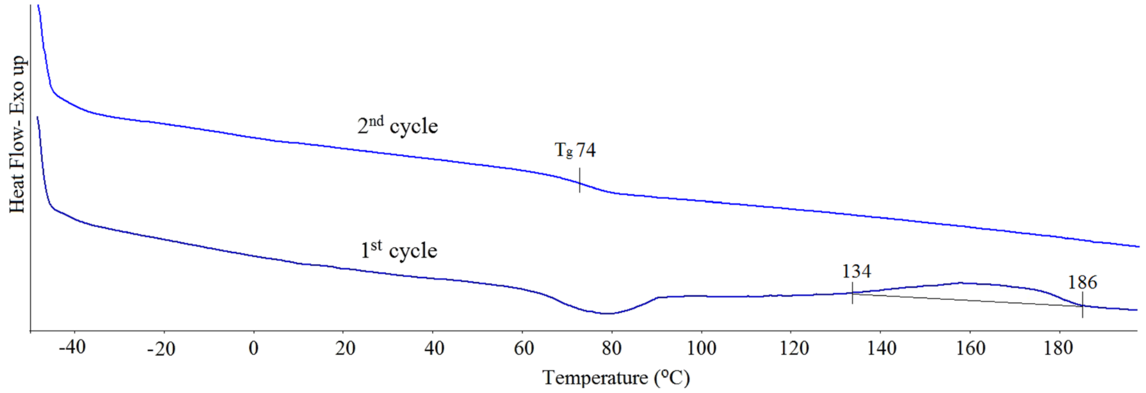

Fig. 5 DSC curve of Pole3S. Unreacted peroxide decomposition starts from 130 °C to 184 °C

Table 2 Multiblock copolymers (100 °C, 5 h, 10 mL toluene)

Code	Pole3S		PoleS11-9		nBMA	Yield	Mn	Mw	‘Đ’ Stress	Strain
	(g)	Mn(Da)	(g)	Mn(Da)	(g)	(g)	(Da)	(Da)	(MPa)	(%)
PoSB-1	0.63	24,700	–	3.4	1.87	30,700	66,000	2.15	10 ± 0.8	17 ± 0.8
PoSB-2	0.63	24,700	–	10.0	4.75	46,000	98,000	2.13	14 ± 0.7	162 ± 12
PoSB-4	–	0.63	10,900	10.0	2.90	59,000	115,000	1.94	15 ± 0.2	133 ± 14
PnBMA-5 (control)						67,900	115,000	1.70	11 ± 0.6	182 ± 30
*PS-10 (control)						107,000	163,000	1.52	15 ± 2.2	4.4 ± 0.3

*Polymerization conditions: AIBN: 0.006 g, Styrene: 20.0 g, Yield: 14.6 g

Table 3 The results and conditions of the condensation reactions between PoleS and PEGNH2 at 110 °C under vacuum for 2 h: chain extension reactions

Code	PoleS		Mn (g/mol)	‘Đ’	PEGNH2 (g)	Yield (g)	PEG in cop.(mol%)	Mn (g/mol)	Mw (g/mol)	‘Đ’
	Type	(g)								
PoleS-11-9PEG-1	PoleS-11–9	1.23	10,900	1.71	1.15	1.10	6	19,600	336,001	1.71
PoleS-6-14PEG-1	PoleS-6–14	1.23	19,400	1.66	1.25	1.13	5	50,400	102,000	2.02
PoleS-2-18PEG-1	PoleS-2–18	1.28	36,100	1.47	1.10	1.10	6	91500	174800	1.91
PoleS2514PEG-3	PoleS-2514	1.04	9400	2.06	1.12	1.02	13	54,400	62,000	1.14

Figure 6 shows the graphical design of the chain extension formation of PoleS-PEG amphiphilic graft copolymer.

In order to understand the influence of the amount of PEGNH2 in the reaction, a series of experiments were carried out. Table 4 contains the results of the condensation reactions of PoleS2514 with varying PEG contents. As the initial feeding of PEGNH2 (wt%) increases from 1.85 to 35.0, the PEG content calculated from the NMR spectra (not given) increased in the copolymer product. The graft copolymer with the maximum PEG content was obtained in the initial feeding of PEG (35wt%). It is expected to limit the carboxylic acid moieties in the PoleS copolymer. After the amidation reactions are completed, the PEG content in the copolymers remained the same. This can be seen in Fig. 7. The yield of the copolymers obtained in the presence of higher PEG contents (PoleS-25-14-PEG-7 and PoleS-25-14-PEG-8 in Table 4) decreased. As the PEG content in the copolymer increases, the properties of the used non-solvent (in this case methanol) improve to the point where additional polymer can be effectively dissolved in the precipitation media thus improving polymer processing. The second point is that the limited carboxylic acid attached to the poly(oleic acid-g-styrene) graft copolymer reacts with the amine terminated PEG. This copolymer reacts with PEGNH2 as much as the attached carboxylic acid groups. Because of this, the PEG in copolymer remains constant. Figure 7 shows the plot of PEG in the copolymers vs PEG in feeding in the condensation reaction between PoleS and PEGNH2.

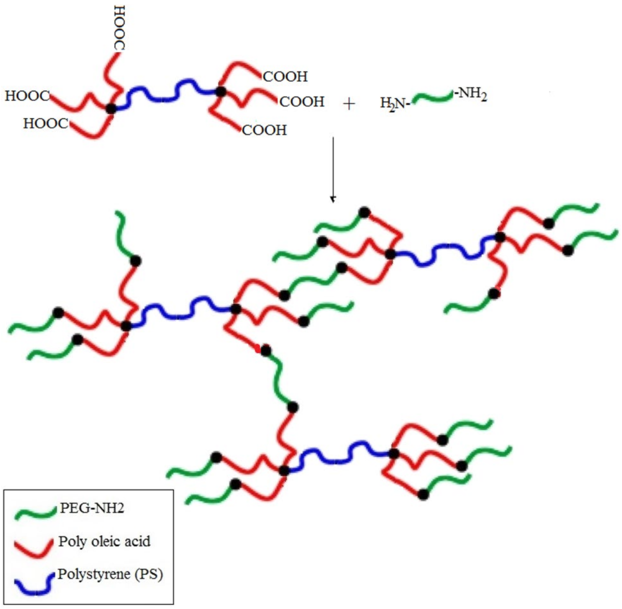

Fig. 6 Schematic representation of the condensation reaction between PoleS with PEGNH2 leading to branched graft copolymer

Table 4 Results and conditions of the condensation reaction of PoleS-2514 with changing amount of PEGNH2

Code	PoleS	PEGNH2		Yield	^{1}H nmr
	(g)	(g)	(wt%)	(g)	(PEG mol%)
PoleS-25–14-PEG-6	1.06	0.020	1.85	1.06	2.2
PoleS-25–14-PEG-3	1.06	0.053	4.8	0.98	3.4
PoleS-25–14-PEG-2	1.06	0.127	10.7	1.00	3.9
PoleS-25–14-PEG-4	1.06	0.250	19.0	1.05	9.0
PoleS-25–14-PEG-7	1.03	0.563	35.0	1.01	13
PoleS-25–14-PEG-8	1.04	0.843	44.8	0.75	12

H and 13C NMR

The products were characterized by taking their ^{1}H and ^{13}C NMR spectra. As typical products, Pole-4m, PoleS-2514, and PoleS-2514-PEG-8 were chosen. ^{1}H NMR and ^{13}C NMR spectra of the samples can be seen in Figs. 8 and 9, respectively. For the oleic acid macroperoxide initiator (Pole-4m), the characteristic signals of the double bond (5.2 ppm in Fig. 8, 128 ppm in Fig. 9) and carboxylic acid proton (broad 8.5 ppm in Fig. 8, 177 ppm for carbonyl in Fig. 9) were observed. Autoxidation resulted in –C–O–. moieties and small signals at 3.2 and 3.9 ppm in Fig. 8, at 70 ppm in Fig. 9 were observed. For Pole-Styrene copolymer (PoleS-2514), characteristic phenyl signals at 6.5 and 7.1 ppm (Fig. 8) and 125–128 ppm (Fig. 9) were observed. Small signals belong to double bond of oleic acid at 5.3 ppm (Fig. 8), 127 ppm (Fig. 9) and methyl group of oleic acid at 0.9 ppm (Fig. 8) and 13 ppm (Fig. 9) were observed. Lastly, characteristic signal of the PEG segment in the oleic acid-styrene-PEG triblock copolymer at 3.7 ppm (Fig. 8) and 70 ppm (Fig. 9) were observed.

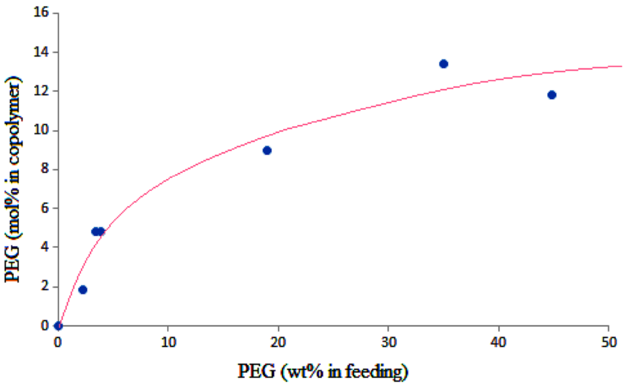

Fig. 7 Plot of PEG in copolymer vs PEG in feeding in the condensation reaction between PoleS and PEGNH2

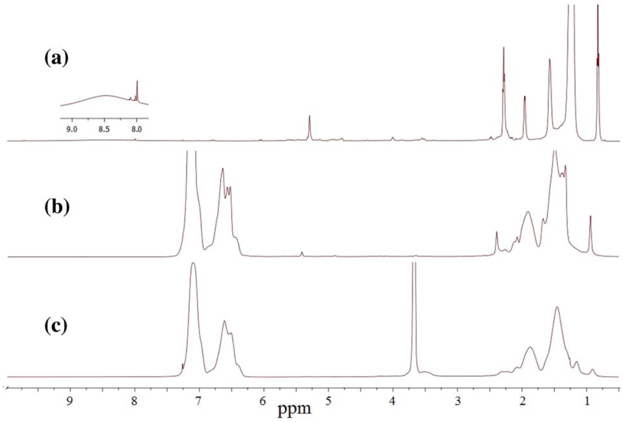

Fig. 8 ^{1}H NMR spectra of **a** Pole-4m, **b** PoleS-2514, and **c** PoleS-2514-PEG-8

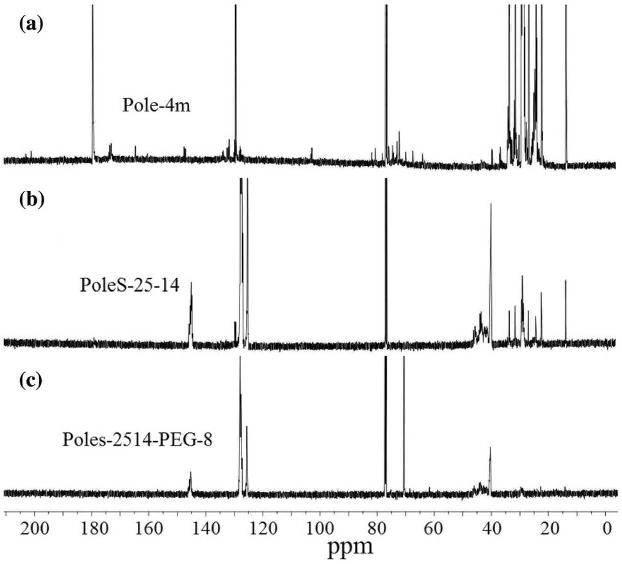

Fig. 9 ^{13}C NMR spectra of **a** Pole-4m, **b** PoleS-2514, and **c** PoleS-2514-PEG-8

One Pot Synthesis of PS-g-Pole-g-PEG Amphiphilic Copolymers

Oleic acid macroperoxide initiator (Pole) was used in the free radical polymerization of styrene (S) in the presence of poly ethylene glycol with two amine ends (PEGNH2) in order to obtain poly(oleic acid-g-styrene-g-PEG) polymer via one pot synthesis. To start the one pot polymerization, a mixture of equimolar ratio of PoleS and PEGNH2 was dissolved in toluene. Salt of $[\text{Pole4m}]^-[\text{ED2003}]^+$ ammonium carboxylate was formed and then styrene was put into this solution to complete the one pot polymerization process at 95 °C. Reaction conditions and molar masses of the produced polymers can be seen in Table 5. Contrary to the bulk condensation reactions, lower molar masses of the graft copolymers with narrow polydispersity were obtained. Moderate water uptake was observed in the copolymers. The ^{1}H NMR spectra of the copolymers show characteristic signals for the PEG, polystyrene and oleic acid moieties (Fig. 10). The PEG contents in the copolymers were calculated using the integral ratio of PEG signal to total integral ratio of the spectrum.

One pot polymerization led to copolymers containing PEG units between 5.7 and 13 mol%. Figure 11 shows a smooth decrease in molar mass as the molar concentration of initiator salt increases and the narrow polydispersities associated with the resultant polymers.

Effect of the Initiator Salt on the Molar Mass of the Copolymers

The higher concentration of the initiator salt caused a decrease in conversion and water uptake. Water uptake of the copolymer increased as PEG content increased. The plots of conversion and water uptake against the concentration of the initiator salt can be seen in Fig. 12.

Table 5 One pot synthesis of poly(oleic acid-g-styrene-g-PEG) (PoSG) copolymers

Code	$[\text{Pole4m}]^-[\text{ED2003}]^+$		S	Yield	Conv	Water up-take	PEG	Mn	Mw	'Đ'
	(g)	(wt%)	(g)	(g)	(wt%)	(wt%)	(mol%)	(g/mol)	(g/mol)	
PoSG-1	2.1	18.75	9.1	2.20	19.6	18	5.7	9900	11,100	1.13
PoSG-2	4.0	33.33	8.0	2.28	19.0	16	6.7	9500	11,700	1.24
PoSG-3	6.0	46.15	7.0	2.07	15.9	25	8.0	6700	8100	1.21
PoSG-4	8.0	56.73	6.1	2.34	16.6	26	15	6100	8700	1.42
PoSG-5	10	66.67	5.0	1.66	11.1	23	14	4800	6700	1.40

Fig. 10 ^{1}H NMR spectra of the obtained polymers by one pot polymerization

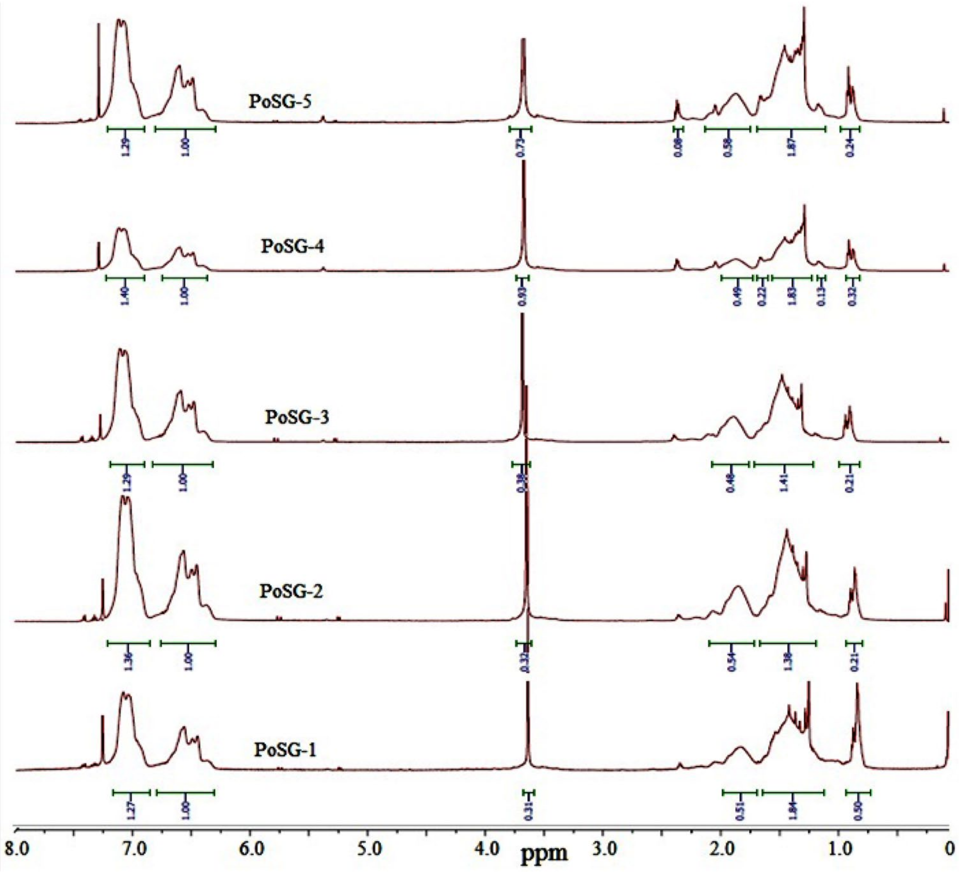

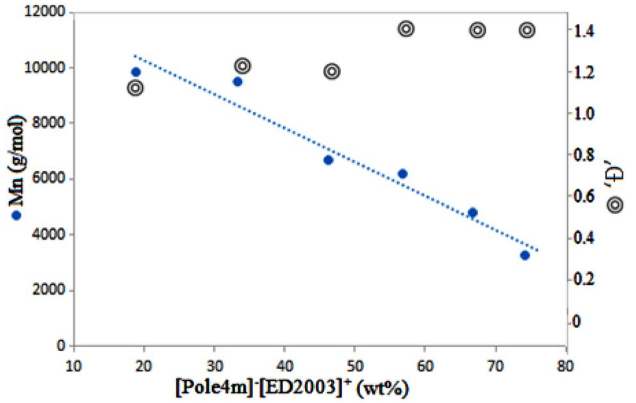

Fig. 11 Plot of the variation of molar masses and polydispersity of the polymers versus the concentration of the initiator salt (Pole PEG ammonium carboxylate)

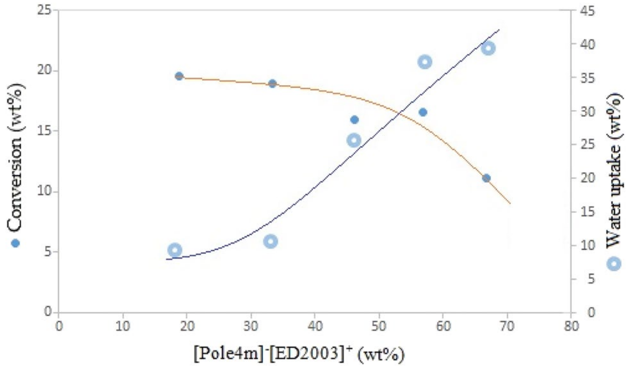

Fig. 12 Plot of the variation of conversion and water uptake of the poly(oleic acid-g-styrene-g-PEG) copolymers versus the concentration of the initiator salt

FTIR

FTIR spectra of the graft copolymers contained the characteristic signals of each segment: Bands (cm^{-1}) at 3060, 3006, 1601, 1492, 1452 for polystyrene, 1713 for Pole and 1099 for PEG were observed. Typical comparative FTIR spectra of the PoleS and the PoSG are shown in Fig. 13.

Thermal Analysis

Thermal analysis of the products was carried out using TGA and DSC techniques. Figure 14 shows the TGA curves of the polymer samples. The starting and point of the decompositions were recorded as Td's. The decomposition temperatures (Td) of the polymers are listed in Table 6. The

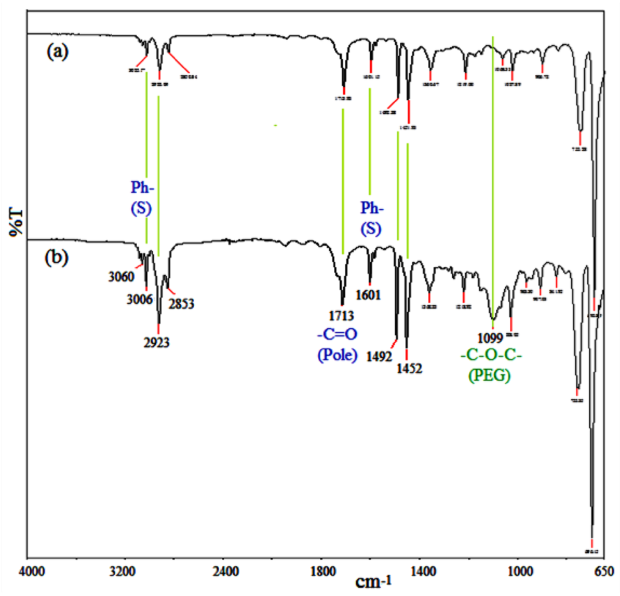

Fig. 13 FTIR spectra of the PoleS (PoleS-6–14 in Table 4) (*a*) and the PoSG (PoleS-6-14PEG-1 in Table 5) (*b*)

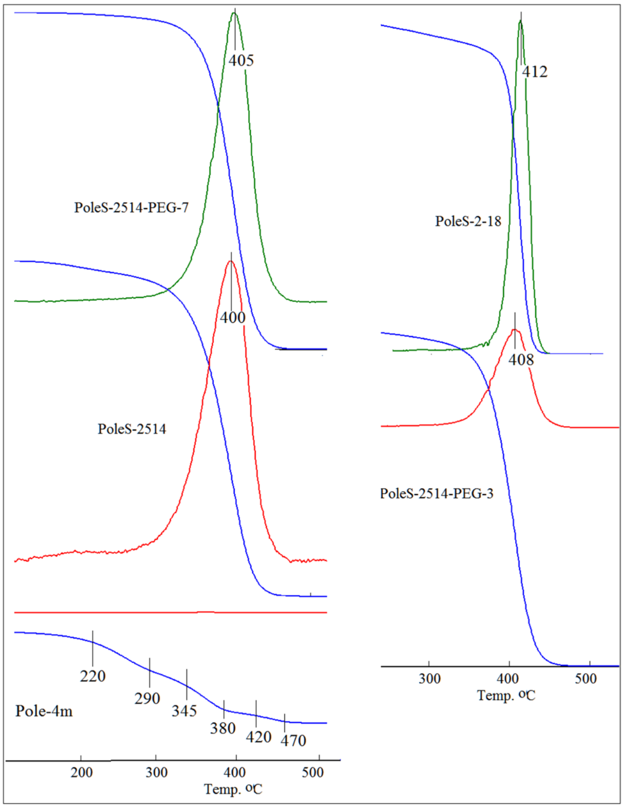

Fig. 14 TGA curves of the polymer samples: **a** Pole4m, **b** PoleS-2-18, **c** PoleS-25–14, **d** PoleS-2514-PEG-3 and **e** PoleS-2514-PEG-7

decomposition of the oleic acid macroperoxide initiator (Pole-4m) was started from 220 °C due to the peroxide groups. The differential thermo gravimetry of the polystyrene copolymers was changing between 400 and 412 °C. The higher poly oleic acid content of PoleS-2514 sample caused the lower decomposition temperature. PEG content was also caused the lower decomposition temperature. The decomposion temperatures of the PoleS graft copolymers decrease slightly with an increase of oleic acid and PEG content in the copolymers.

Figure 15 shows the DSC curves of the copolymer samples. Because of the plasticizer effect of the oleic acid, the higher oleic acid content of PoleS2514 (a), led to the lower Tg (65 °C) when compared to PoleS-2-18 which had a lower oleic acid content. The Tg values of the PoSG copolymers, c and d, stayed the same in spite of varying PEG content.

Morphology of the Copolymers

Fracture surface morphology of the copolymers was studied by SEM technique. Agglomerations of PEG blocks in copolymer matrix were observed in poly(oleic acid-g-styrene-g-PEG) samples (PoSG series). The homogenous spherical PEG aggregations with size around 15 nm can be seen in Fig. 16.

A series of poly(oleic acid-g-styrene) diblock copolymers (PoleS series) showed a fibrillar structure with a smooth continuous matrix. A typical SEM image of the diblock copolymer, PoleS-2-18, can be seen in Fig. 17.

The turbid solution was used for TEM analysis to observe micelle formation of PoSG amphiphilic graft copolymer. Figure 18 shows the TEM micrographs of PoSG-3 in turbid solution of THF/H_2O. The micelles were almost spherical with a size of approximately 100 nm as shown in Fig. 18a. A magnified micelle image is seen in Fig. 18b which shows the core of the PEG blocks confined by a poly(oleic acid-g-styrene) diblock hydrophobic corona.

Stress–Strain Measurements

The results of stress–strain measurements of Pole4m-g-PS diblock copolymers and homoPS can be seen in Table 7. The inclusion of oleic acid made the copolymer tougher than the homopolymer. Figure 19 shows the variation of the stress–strain values against feeding concentration of poly(oleic acid) in the series of the Pole4m-g-PS diblock copolymers.

Table 6 Thermo gravimetric analysis of the polymers obtained

Polymer	T_{d1} (°C)		T_{d2} (°C)		T_{d3} (°C)		T_{max} (°C)
Sample	Start	End	Start	End	Start	End	(dtg)
Pole-4m	220	290	345	380	420	470	Not determined
PoleS-2-18	–	–	380	430	–	–	412
PoleS-2514	–	–	270	375	–	–	400
PoleS-2514PEG-3	–	–	260	390	400	490	408
PoleS-2514PEG-7	–	–	305	405	410	490	405

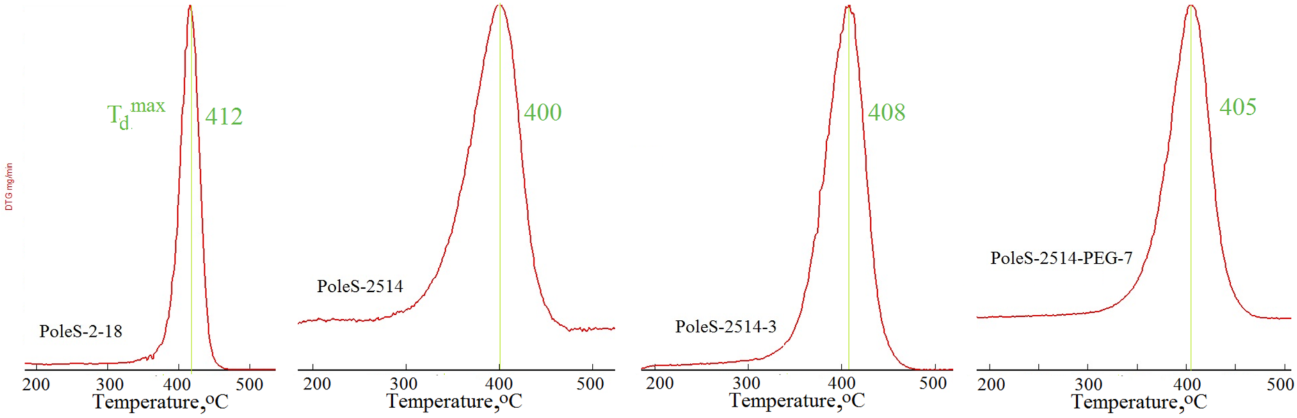

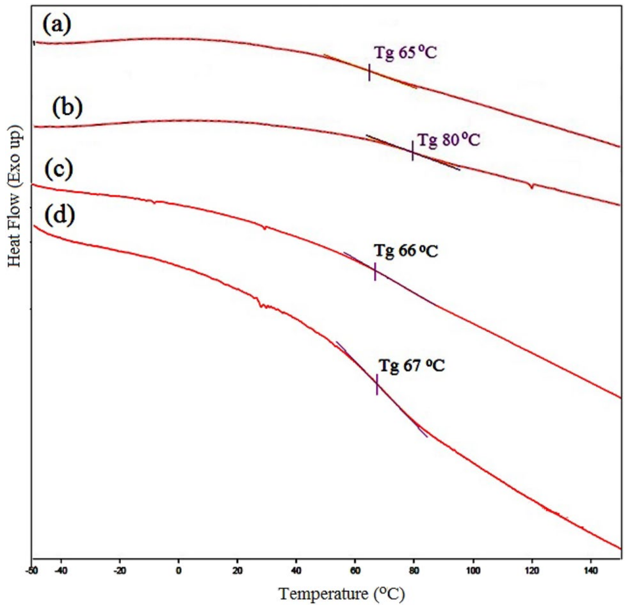

Fig. 15 DSC curves of copolymer samples: *a* PoleS-2514, *b* PoleS-2-18, *c* PoleS2514-PEG-7 and *d* PoleS2514-PEG-3

Conclusion

Autoxidation is a useful tool to produce derivatives of unsaturated vegetable oils and fatty acids. Ecofriendly autoxidation does not need extra energy, extra reagent or extra irradiation and leads to formation of macroperoxide initiators for free radical polymerization. The fatty acid macroperoxide initiators open a new route to produce polymers with alternative topology and versatile graft copolymers because of their carboxylic acid and peroxide functionalities. Oleic acid macroperoxide initiator obtained in the first stage of this work was an excellent free radical initiator for olefin polymerization and one pot synthesis of multiblock copolymers. The structural characterization of the oleic acid peroxy initiator was simpler than that of the linolenic and linoleic acid macroperoxides. In addition, in the case of the oleic acid macroperoxide initiator, the higher polymerization

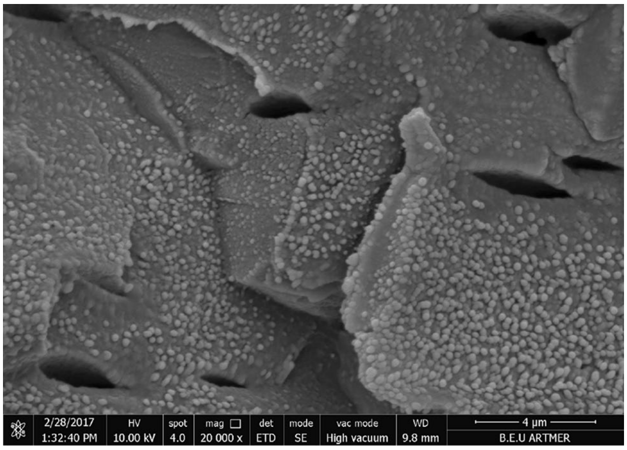

Fig. 16 SEM fractured surface micrograph of the amphiphilic polymer PoSG-3

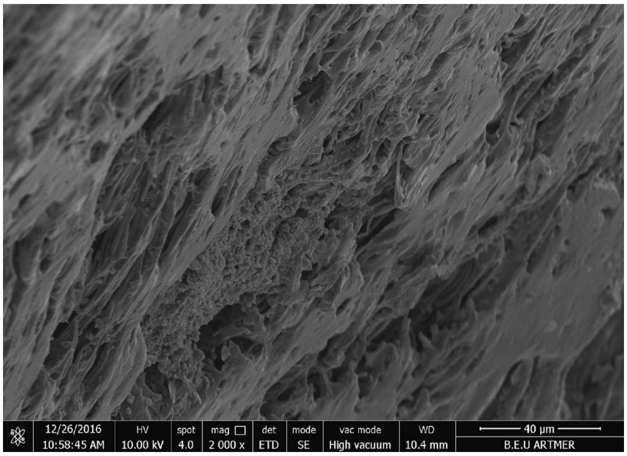

Fig. 17 SEM fractured surface micrograph of a diblock copolymer, PoleS-2-18

temperatures (e.g. 95 °C) led to a high yield of graft copolymer without crosslinking while the polyunsaturated fatty acids were polymerized at lower temperatures (e.g. 80 °C) in order to avoid crosslinking. As a result, we have completed the autoxidation of soybean oil and its fatty acids separately and confirmed both soybean oil and unsaturated fatty acid autoxidation lead to the formation of macroperoxide initiator in order to obtain partially green graft copolymers. Another advantage of using oleic acid is the less-complicated autoxidation and graft copolymerization due to the presence of only one double bond and two allylic groups for peroxide formation.

Narrow molar masses of the novel amphiphilic graft copolymers can be obtained by this method. These materials can be used as biomaterials in drug delivery systems and tissue engineering. The plasticized effect of oleic acid

Table 7 Mechanical properties of the Pole4m-g-PS diblock copolymers

Code	Stress (MPa)	Strain (%)
Pole4mS-1	21.8 ± 3.2	6.4 ± 1.8
Pole4mS-4	30.6 ± 4.7	8.8 ± 4.0
Pole4mS-5	30.6 ± 4.3	6.6 ± 2.4
Pole4mS-6	29.2 ± 2.1	6.3 ± 0.9
Pole4mS-7	21.6 ± 1.8	8.0 ± 0.9
Pole4mS-9	23.7 ± 2.3	7.9 ± 2.2
Pole3S	25.0 ± 3.8	7.8 ± 0.7
PS-10	15.0 ± 2.2	4.4 ± 0.3

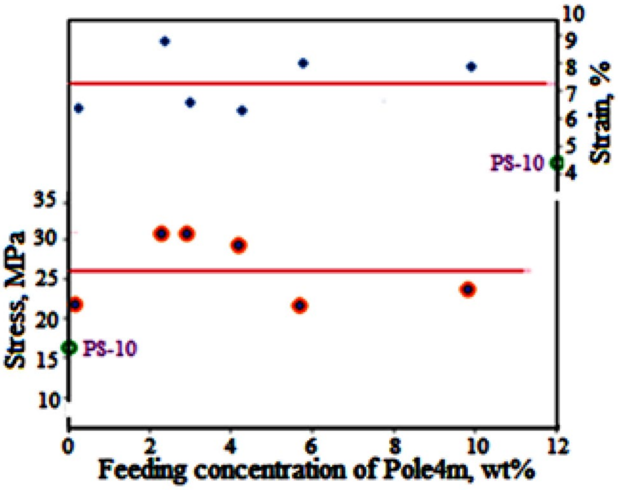

Fig. 19 Variation of stress–strain values against feeding concentration of poly(oleic acid) in the series of the Pole4m-g-PS diblock copolymers

Fig. 18 TEM micrograph of the THF/H_2O turbid solution of the amphiphilic graft copolymer, PoSG-3. Scale bars **a** 1000 nm and **b** 500 nm

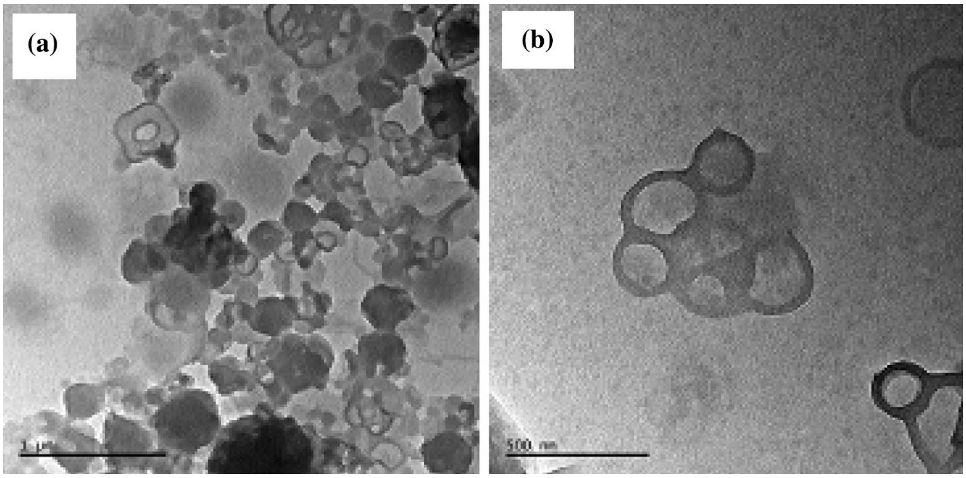

leads to improved mechanical properties. Because of these properties, the polymeric materials obtained can be promising materials in the application of tissue engineering and industry.

Acknowledgements This work was supported by the Kapadokya University Research Fund (KÜN.2018-BAGP-001) and Bülent Ecevit University Research Fund (#BEU-2017-72118496-01). The Authors thank to Koray Alper and Fatih Pekdemir for taking SEM and FTIR spectra, respectively. The Authors thank to Serdar Çoban, Sıdıka Saraç Tabaklı and Gülşen Darıcı (Cilas Kauçuk, Devrek, Zonguldak, Turkey) for taking stress–strain measurements.

Compliance with Ethical Standards

Conflict of interest There is not any conflict of interest.

References

1. Reddy MM, Vivekanandhan S, Misra M, Bhatia SK, Mohanty K (2013) Biobased plastics and bio nanocomposites: Current status and future opportunities. Prog Polym Sci 38:1653–1689
2. Miyaji H, Satoh K, Kamigaito M (2016) Bio-based polyketones by selective ring-opening radical polymerization of a-pinene-derived pinocarvone. Angew Chem Int Ed 55:1372–1376
3. Sudesh K, Iwata T (2008) Sustainability of biobased and biodegradable plastics. CLEAN 36:433–442
4. Shimada K, Fujikawa K, Yahara K, Nakamura T (1992) Antioxidative properties of xanthan on the autoxidation of soybean oil in cyclodextrin emulsion. J Agric Food Chem 40:945–948
5. Khan S, Wang Z, Wang R, Zhang L (2016) Synthesis and structure design of new bio-based elastomers via Thiol-ene-Click Reactions. Mater Sci Eng C 67:554–560
6. Miao S, Wang P, Su Z, Zhang S (2014) Vegetable-oil-based polymers as future polymeric biomaterials. Acta Biomater 10:1692–1704
7. Guner FS, Yagci Y, Erciyes AT (2006) Polymers from triglyceride oils. Prog Polym Sci 31:633–670
8. Sharma BK, Adhvaryu A, Erhan S (2006) Synthesis of hydroxy thioether derivatives of vegetable oil. J Agric Food Chem 54:9866–9872
9. Wang Z, Zhang X, Wang R, Kang H, Qiao B, Ma J, Zhang L, Wang H (2012) Synthesis and characterization of novel soybean-oil-based elastomers with favorable processability and tunable properties. Macromolecules 45:9010–9019
10. Hazer DB, Hazer B (2009) Kaymaz F (2009) Synthesis of microbial elastomers based on soybean oily acids. Biocompat Stud Biomed Mater 4:035011
11. Petrović ZS, Zhang W, Javni J (2005) Structure and properties of polyurethanes prepared from triglyceride polyols by ozonolysis. Biomacromol 6:713–719
12. Narine SS, Kong XH, Bouzidi L, Sporns P (2007) Physical properties of polyurethanes produced from polyols from seed oils: I. Elastomers. J Am Oil Chem Soc 84:55–63
13. Porter NA (2013) A perspective on free radical autoxidation: the physical organic chemistry of polyunsaturated fatty acid and sterol peroxidation. J Org Chem 78:3511–3524
14. Soucek MD, Khattab T, Wu J (2012) Review of autoxidation and driers. Prog Org Coat 73:435–454
15. Hamalainen TI, Sundberg S, Makinen M, Kaltia S, Hase T, Hopia A (2001) Hydroperoxide formation during autoxidation of conjugated linoleic acid methyl ester. Eur J Lipid Sci Technol 103:588–593
16. Yin H, Xu L, Porter NA (2011) Free radical lipid peroxidation: Mechanisms and analysis. Chem Rev 111:5944–5972
17. Choe E, Min DB (2006) Mechanisms and factors for edible oil oxidation. Compr Food Sci Food Saf 5:169–186
18. Mcclements DJ, Decker EA (2000) Lipid oxidation in oil-in-water emulsions: Impact of molecular environment on chemical reactions in heterogeneous food systems. J Food Sci 65:1270–1282
19. Köckritz A, Martin A (2008) Oxidation of unsaturated fatty acid derivatives and vegetable oils. Eur J Lipid Sci Technol 110:812–824
20. Ionescu M, Petrović ZS, Wan X (2007) Ethoxylated soybean polyols for polyurethanes. J Polym Environ 15:237–243
21. Fornof AR, Onah E, Ghosh S, Frazier CE, Sohn S, Wilkes GL, Long TE (2006) Synthesis and characterization of triglyceride-based polyols and tack-free coatings via the air oxidation of soy oil. J Appl Polym Sci 102:690–697
22. Montero de Espinosa L, Ronda JC, Galia M, Cadiz VA (2009) New route to acrylate oils: Crosslinking and properties of acrylate triglycerides from high oleic sunflower oil. J Polym Sci A 47:1159–1167
23. Keleş E, Hazer B (2009) Synthesis of segmented polyurethane based on polymeric soybean oil polyol and poly (ethylene glycol). J Polym Environ 17:153–158
24. Acar M, Çoban S, Hazer B (2013) Novel water soluble soya oil polymer from oxidized soya oil polymer and diethanol amine. J Macromol Sci A 50:287–296
25. Hazer B, Akyol E (2016) Efficiency of gold nano particles on the autoxidized soybean oil polymer. Fractionation and structural analysis. J Amer Oil Chem Soc 93:201–213
26. Hazer B, Kalaycı ÖA (2017) High fluorescence emission silver nano particles coated with poly (styrene-g-soybean oil) graft copolymers: antibacterial activity and polymerization kinetics. Mater Sci Eng C 74:259–269
27. Yıldız U, Hazer B, Tauer K (2012) Tailoring Polymer Architectures with Macromonomer azoinitiators. Polym Chem 3:1107–1118
28. Erciyes AT, Erim M, Hazer B, Yağcı Y (1992) Synthesis of polyacrylamide flocculants with PEG segments by redox polymerization. Angew Macromol Chem 200:163–171
29. Yıldız U, Hazer B (2000) Dispersion redox copolymerization of methyl methacrylate with macromonomeric azoinitiator as a macrocrosslinker. Polymer 41:539–544
30. Hazer B (1987) Polymerization of vinyl monomers by a new oligoperoxide. Oligo (adipoyl 5- peroxy 2,5- dimethyl n-hexyl) peroxide. J Polym Sci Polym Chem Ed 25:3349–3354
31. Öztürk T, Yılmaz SS, Hazer B (2008) Synthesis of a new macroperoxy initiator with methyl methacrylate and t-butyl peroxy ester by atom transfer radical polymerization and copolymerization with conventional vinyl monomers. J Macromol Sci Part A 45:811–820
32. İnce Ö, Akyol E, Sulu E, Şanal T, Hazer B (2016) Synthesis and characterization of novel rod-coil (tadpole) poly(linoleic acid) based graft copolymers. J Polym Res 23:1–10
33. Allı A, Allı S, Becer CR, Hazer B (2016) Nitroxide mediated copolymerization of styrene and pentafluorostyrene initiated by polymeric linoleic acid. Eur J Lipid Sci Tech 118:279–287
34. Hazer B, Ayyıldız E, Bahadır F (2017) Synthesis of PNIPAM-PEG double hydrophilic polymers using oleic acid macro peroxide initiator. J Am Oil Chem Soc 94:1141–1151
35. Hazer B (2010) Amphiphilic poly (3-hydroxy alkanoate)s: potential candidates for medical applications. Int J Polym Sci. https://doi.org/10.1155/2010/423460
36. Hutanu D, Frishberg MD, Guo L, Darie CC (2014) Recent applications of polyethylene glycols (pegs) and peg derivatives. Modern Chem Appl 2:132. https://doi.org/10.4172/2329-6798.1000132

37. Hazer DB, Mut M, Dinçer N, Sarıbaş Z, Hazer B, Özgen T (2012) The efficacy of Ag embedded pp-g-peg coated ventricular catheters on prevention of shunt catheter infection in rats. Childs Nerv Syst 28:839–846
38. Hazer B (1995) Grafting on polybutadiene with macro or macromonomer initiator containing poly(ethylene glycol) units. Macromol Chem Phys 196:1945–1952
39. Townsend KJ, Busse K, Kressler J, Scholz C (2005) Contact angle, WAXS, and SAXS analysis of poly(β-hydroxybutyrate) and poly(ethylene glycol) block copolymers obtained via *Azotobacter vinelandii* UWD. Biotechnol Prog 21:959–964
40. Charoongchit P, Suksiriworapong J, Sripha K, Mao S, Sapin-Minet A, Maincent P, Junyaprasert VB (2017) Self-aggregation of cationically modified poly(ε-caprolactone)2-co-poly(ethylene glycol) copolymers: Effect of cationic grafting ligand and poly(ε-caprolactone) chain length. Mater Sci Eng C 72:444–455
41. Gody G, Rossner C, Moraes J, Vana P, Maschmeyer T, Perrier S (2012) One-pot RAFT/"click" chemistry via isocyanates: efficient synthesis of α-end-functionalized polymers. J Am Chem Soc 134:12596–12603
42. Wang S, Fu C, Zhang Y, Tao L, Li S, Wei Y (2012) One-pot cascade synthetic strategy: a smart combination of chemo enzymatic transesterification and raft polymerization. ACS Macro Lett 1:1224–1227
43. Geng J, Lindqvist J, Mantovani G, Haddleton DM (2008) Simultaneous copper(i)-catalyzed azide–alkyne cycloaddition (cuaac) and living radical polymerization. Angew Chem Int Ed 47:4180–4183
44. Yagci Y (1985) Block copolymers by combinations of cationic and radical radical routes. 1. A new difunctional azo-oxocarbenium initiator for cationic polymerization. Polym Commun 26:7–8
45. Hazer B (1991) Synthesis of tetrahydrofuran-styrene (or methyl methacrylate) block copolymers via cationic to radical transformation process. Eur Polym J 27:775–777
46. Hazer B (1990) Cationic polymerization of tetrahydrofuran initiated by difunctional initiators. Synthesis of block copolymers. Eur Polym J 26:1167–1170
47. Hazer B (1991) Synthesis of styrene-tetrahydrofuran branched block copolymers. Eur Polym J 27:975–978
48. Mazurowski M, Gallei M, Li J, Didzoleit H, Stühn B, Rehahn M (2012) Redox-responsive polymer brushes grafted from polystyrene nanoparticles by means of surface-initiated atom transfer radical polymerization. Macromolecules 45:8970–8981
49. Díaz I, Langston P, Ovejero G, Romero MD, Díez E (2010) Purification process design in the production of styrene monomer. Chem Eng Process 49:367–375
50. Firestone D (1994) Determination of the iodine value of oils and fats: summary of collaborative study. JAOAC Int 77:674–676
51. Brimberg UI, Kamal-Eldin A (2003) On the kinetics of the autoxidation of fats: substrates with conjugated double bonds. Eur J Lipid Sci Technol 105:17–22
52. Porter NA, Mills KA, Carter RL (1994) A mechanistic study of oleate autoxidation: competing peroxyl h-atom abstraction and rearrangement. J Am Chem Soc 116:6690–6696
53. Knothe G, Kenar JA (2004) Determination of the fatty acid profile by ^{1}H-NMR spectroscopy. Eur J Lipid Sci Technol 106:88–96
54. Guillén MD, Ruiz A (2005) Study by proton nuclear magnetic resonance of the thermal oxidation of oils rich in oleic acyl groups. J Am Oil Chem Soc 82:349–355
55. Hwang H-S, Doll KM, Winkler-Moser JK, Vermillion K, Liu SX (2013) No evidence found for diels–alder reaction products in soybean oil oxidized at the frying temperature by NMR study. J Am Oil Chem Soc 90:825–834
56. Matyjaszewski K, Spanswick J (2005) Controlled/living radical polymerization. Mater Today 8:26–33
57. Hazer B (1996) Poly(beta-hydroxynonanoate) and polystyrene or poly(methyl methacrylate) graft copolymers: microstructure characteristics and mechanical and thermal behavior. Macromol Chem Phys 197:431–441
58. Cakmakli B, Hazer B, Borcakli M (2001) Poly(styrene peroxide) and poly(methyl methacrylate peroxide) for grafting on unsaturated bacterial polyesters. Macromol Biosci 1:348–354